Cross Sections for Products of 90-Mev Neutrons on Carbon*

D. A. Kellogg†

Department of Physics, University of California, Berkeley, California

(Received December 29, 1952)

Determinations have been made of the cross sections for the products of 90-Mev neutrons on carbon in the case of practically all reactions that occur. Beta-counting of the activities generated in a rotating polyethylene disk yielded cross sections for the production of some heavy fragments, identified as to isotope and atomic number. Cloud-chamber study yielded cross sections for almost all reactions, but resulted in the identification of most of the heavy fragments only by atomic number. The rotating disk method cross sections were normalized to the $C^{12}(n;2n)C^{11}$ cross section, and the cloud-chamber method cross sections were normalized to the $n-p$ cross section.

I. INTRODUCTION

THE symmetric nuclear constitution and possible α-particle substructure of carbon 12 make its nuclear reactions hold special interest. In particular, reactions of carbon with 90-Mev neutrons are studied because the theory of the compound nucleus is not valid at this energy, and information may be gained concerning knock-on interactions and spallations.

The object of this work was to determine relative and absolute cross sections, as far as possible, for all reactions that occur in carbon bombarded by 90-Mev neutrons. The general plan was to accept the present values of the cross sections for the two following processes:

(1) $C^{12}(n;2n)C^{11}$ cross section $= 22\pm4$ millibarns.[1]

(2) $n-p$ scattering cross section $= 77\pm1.5$ millibarns.[2-5]

These values were used to normalize all cross sections to absolute values. The 90-Mev neutrons used in bombarding carbon were produced by 190-Mev deuteron bombardment of a half-inch beryllium target (Serber stripping[6]) in the 184-inch cyclotron. The resulting neutrons have an energy spectrum measured experimentally[3,7] as having a peak with a maximum at about 90 Mev, and a half-width of 25 to 30 Mev.

II. PRINCIPLES OF EXPERIMENTAL METHODS

The two methods employed to identify reaction products and measure cross sections were (1) identification and counting of the beta-particle activities of the heavy residual nuclei produced from carbon; (2) identification and counting of the prongs of carbon stars photographed in a cloud chamber.

The beta-activity method identified and counted specific isotopes of heavy residual nuclei, but gave no direct information about light fragments. The cloud-chamber method identified and counted light fragments by isotope, but identified heavy, residual nuclei only by atomic number in most cases. The two methods were therefore complementary.

A. The Beta-Activity (Rotating Disk) Method

Following the design principle used by Becker and Gaerttner,[8] a rotating disk of polyethylene was bombarded at one circular area near the rim by a well collimated neutron beam of 90-Mev neutrons. This process quickly built up equilibrium concentrations of each of the short-lived beta-activities that are generated from carbon. These concentrations had a steady value (assuming constant speed, uniform disk thickness, and a neutron beam of uniform time and position intensity) at each point of the disk as that point reached a given angular position in rotation. This meant that manually-timed counts of minutes' duration could be taken at given angular positions on activities whose half-lives are quite short (0.025 to 0.88 second), provided that the equilibrium was maintained. A plot of activity against angular position was then equivalent to the usual plot of activity against time made for artificially radioactive samples counted after bombardment instead of during bombardment. A complicating factor was the gradual build-up of any activity whose half-life is of the order of or longer than the time used for "warm-up" to equilibrium. In this case the $C^{12}(n;2n)C^{11}$ beta-activity ($T_{\frac{1}{2}} = 20.5$ minutes) required a determination of the build-up rate of this activity and correction of every counter reading by subtraction of the appropriate C^{11} activity.

The C^{11} activity furnished the essential normalization needed to place measured cross sections on an absolute scale, since the C^{11} cross section is known. However, since the various beta-activities produced in carbon

[1] E. McMillan and H. York, Phys. Rev. 73, 262 (1948).
[2] J. Hadley and H. York, Phys. Rev. 80, 345 (1950).
[3] Hadley, Kelly, Leith, Segrè, Wiegand, and York, Phys. Rev. 75, 351 (1949).
[4] J. de Juren and N. Knable, Phys. Rev. 77, 606 (1950).
[5] Cook, McMillan, Peterson, and Sewell, Phys. Rev. 72, 1264 (1947).
[6] R. Serber, Phys. Rev. 72, 1008 (1947).
[7] Brueckner, Hartsough, Hayward, and Powell, Phys. Rev. 75, 555 (1949).

[8] R. A. Becker and E. R. Gaerttner, Phys. Rev. 56, 854 (1939).

have maximum beta-energies ranging from 1 to 13 Mev, a determination of self-absorption factors was necessary to determine true relative production ratio. This was done by using disks of varying thicknesses and extrapolating their activities to that of zero-thickness disks.

The separation of the beta activities present was facilitated by using several rotation speeds; a given activity could be brought into relative predominance over others at certain angular positions by making the rotation speed roughly equal to the mean life of the activity in question. The longer lived activities could also be counted conventionally; i.e., with the neutron beam turned off. Selective beta-absorption could be used to separate activities whose half-lives are nearly identical—provided the beta-energy end points differ sufficiently.

B. The Cloud-Chamber Method

This method of study consisted of passing a pulsed, collimated 90-Mev neutron beam through a large cloud chamber placed in a high magnetic field and filled with a mixture of methane and hydrogen gasses. The cloud chamber was expanded shortly before each pulse, and a stereoscopic pair of photographs was taken shortly after the pulse. The photographs were examined through a stereoscopic viewer and also reprojected onto a glass plate as life-size, three-dimensional images. The inelastic interactions of neutrons with carbon were seen as stars of two or more prongs. The individual prongs, or fragment tracks, were identified by using radius of curvature, specific ionization, and range.

III. ROTATING DISK BETA METHOD

The rotating disk apparatus consisted basically of interchangeable polyethylene disks of 21-inch diameter rotated by electric motors at speeds monitored by a stroboscope. High counting background during beam-on operation required good collimation of the neutron beam; this was attained with a two-inch diameter collimator six feet long, surrounded by lead and concrete of a minimum thickness of six feet, placed 30 feet from the beryllium target. The resulting beam was about 3.3 inches in diameter as it passed perpendicularly through the outer periphery of the disk.

A cross arm pivoted on the trunnions of the apparatus supported four heavy lead shields, each of which contained a Tracerlab TCG-1 end-window Geiger-Muller counter. The shields provided two inches of lead on all sides of the counters except over the windows, which were set back one-half inch from the faces of the shields, adjacent to the polyethylene disk. The face-plate of each shield had a hole the size of the counter window, with a 45 degree outward flare the outermost quarter of an inch. This construction provided a partial telescope for the beta-particles, and was chosen by trial and error for the purpose of equalizing counting geometry as much as possible for betas of varying maximum energies.

TABLE I. Possible radioactive products of carbon.

Isotope	Activity	Half-life	Maximum beta energy (Mev)	Remarks	Ref.
B^{12}	β^-	0.025 sec	13.46		a
Li^9	β^-	0.168 sec	11		b
B^8	β^+	0.65 sec	13.7		c
He^6	β^-	0.87 sec	3.7	no γ	d
Li^8	β^-	0.89 sec	12.7	no γ	a
C^{10}	β^+	19.1 sec	2.2	γ 0.96 Mev	e
C^{11}	β^+	20.5 min	0.98	no γ	f
Be^7	K-capture	52.93 day	0.48 (γ)	one γ per 10.7 disint.	g
Be^{10}	β^-	2.5×10^6 yr	0.56	no γ	h

a W. Hornyak and T. Lauritsen, Phys. Rev. 77, 160 (1950).
b N. Knable, Phys. Rev. 83, 1054 (1951).
c L. Alvarez, Phys. Rev. 80, 519 (1951).
d R. Latham, Nature 159, 367 (1947).
e Sherr, Muether, and White, Phys. Rev. 75, 282 (1949).
f A. Solomon, Phys. Rev. 60, 279 (1941).
g E. Segrè and C. Wiegand, Phys. Rev. 75, 39 (1949).
h E. McMillan, Phys. Rev. 72, 591 (1947).

The counters were mounted in two pairs 180 degrees apart and facing one another, with the pairs of lead face plates one-half inch apart. The disk rotated midway between each pair of face plates.

Detailed theoretical consideration of the beta-activity counting rates to be expected was required to test the feasibility of using the rotating disk method to separate and measure the activities whose presence was known or suspected.

It was, therefore, necessary to derive the expression for expected counting rate of an activity of sufficiently short half-life to reach equilibrium in a minute or less, modify this expression to encompass longer-lived activities not expected to reach equilibrium, and take a ratio of these two expressions as follows:

$$\frac{C(\theta_0)}{C_C} \approx \frac{\sigma_B \epsilon_B}{\sigma_C \epsilon_C}\left(\frac{\lambda_B}{2\pi\omega}\right)\left(\frac{1-e^{-\lambda_C t}}{1-e^{-2\pi\lambda_B/\omega}}\right)e^{-\lambda_B\theta_0/\omega}, \quad (1)$$

where ω is the angular speed of rotation of the disk, σ is the cross section for formation of the active nuclei considered, λ is the disintegration constant of the activity considered ($\lambda_B = \lambda$ of boron 12, $\lambda_C = \lambda$ of carbon 11), ϵ is the counting efficiency of the counter for the activity in question (including solid angle corrections), $C(\theta_0)$ is the short half-life activity counting rate at angular position θ_0 of the counter with respect to the neutron beam, and C_C is the carbon 11 activity present at the same time.

The quantities $\epsilon_{B^{12}}$ and $\epsilon_{C^{11}}$ were never determined absolutely, but this was not considered necessary since only the ratio $\epsilon_{B^{12}}/\epsilon_{C^{11}}$ occurs in Eq. (1). The only plausible difference between $\epsilon_{B^{12}}$ and $\epsilon_{C^{11}}$ occurs because of the difference in beta-energies of the two activities; the boron 12 beta-spectrum has a maximum energy of 13.4 Mev, while the carbon 11 beta-spectrum has a maximum energy of 0.98 Mev. Aside from the differing self-absorption (in the polyethylene) factors involved,
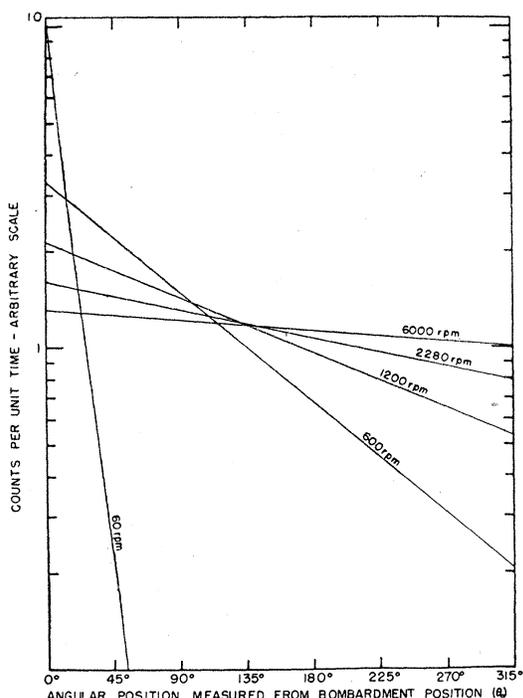
FIG. 1. Theoretical B^{12} beta-activity at various disk rotation speeds, plotted as a function of the angular position of the counter with respect to the neutron beam.

this presented the problem of making a counter geometry that would be not too dissimilar for high and low energy betas. The counter-shield design was such as to present either a clear air path to any incident betas, or else a path filled with enough lead to stop all betas up to 14 Mev, with a minimum transition between the two conditions. Therefore, only self-absorption, air-path
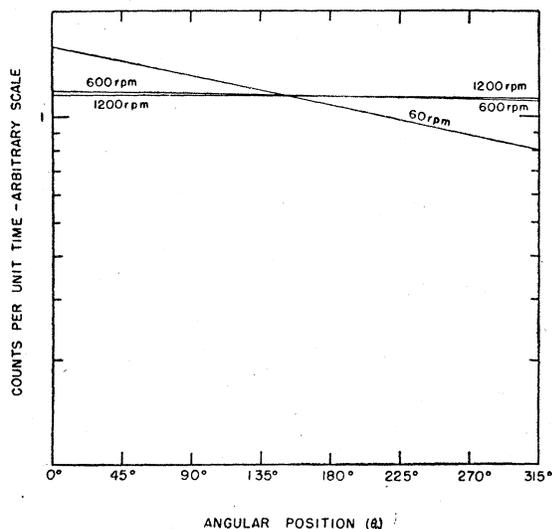
FIG. 2. Theoretical $Li^8 + He^6$ beta-activity at various disk rotation speeds as a function of counter angular position.

absorption, and counter-window absorption were taken into account for computing the ratio.

Search of the literature produced a list of the possible activities that might be generated, as given in Table I.

The logical plan of attack was the physical separation of these activities by variation of disk speed and delayed counting. Figure 1 shows a plot to an arbitrary scale of B^{12} activity for various speeds, and Fig. 2 shows the same plot for Li^8 and/or He^6 activity.

At 60 rpm, B^{12} activity decreased vanishingly beyond angular counting position 45°, while the Li^8 and/or He^6 activities remained fairly high. Figure 3 shows what counting rate might be expected from a mixture of these activities (5 millibarns of B^{12} plus 3 millibarns of Li^8
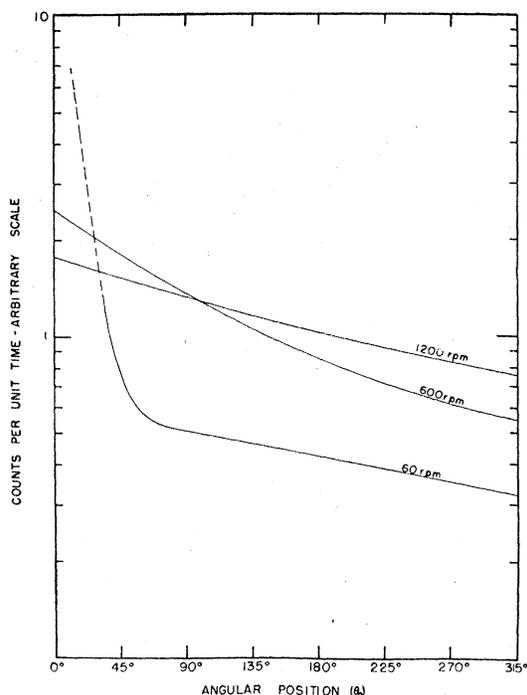
FIG. 3. Theoretical $B^{12} + Li^8 + He^6$ beta-activity at various disk rotation speeds as a function of counter angular positions.

and/or He^6) at various speeds. Changes in slope and height of the plotted counting rate curves (for equilibrium condition) with disk speed indicated a possible way to separate some of the activities present and give, at least, estimates of the amounts present of others.

Numerous runs were made with the disk rotating at various speeds, with single and double thickness disks, with stationary disks, with and without absorbers in front of the counters.

Each activity counting rate was used to correct the counting rate of the next shorter half-life activity in the same general manner that a plot of a mixture of activities is broken down into its component activities. In this case, however, the actual counting rate of a given short-lived activity determined in a run at one

speed had to be converted to the rate this activity would have had at a second speed before being used to correct a run made at that second speed. Figure 4 shows a typical 600-rpm run, plotted on a semilogarithmic scale. The top curve is the raw data, reduced to counts per minute, taken at various angular positions referenced to the position of the neutron beam. The second curve has been corrected by subtracting the beam-on background and C^{11} activity. The third curve down has been corrected for $(Li^8 + He^6 + C^{11})$ activity as described above. This is the B^{12} beta-activity curve. Beam intensity corrections were made to all the data in advance in order to eliminate the beam-variation distortion from each of the curves shown. Figure 5 shows similar curves for a 60-rpm run.

The C^{11} activity count was relatively easy to obtain. One minute after the neutron beam was turned off, all the activities except C^{11} had become negligible. A ten-minute count was taken, and then a second ten-minute count was taken to verify the fact that no other activity was detectable. Background runs taken with no beam and a fresh disk were used to subtract out normal cosmic ray effect. After background correction, the second count matched the first to within statistical error upon being corrected for the decay of C^{11} between the two counts.

The C^{10} activity was counted by connecting a Brush recorder to the register input of one or two counters just as the beam was turned off. Within three seconds, the B^{12}, Li^8, and He^6 activities were essentially gone, and only C^{10} and C^{11} activities were left. (Be^7 activity was quite low since this is a gamma-activity, and was practically constant because of its long half-life.) The count rate for the first minute was compared with the rate for the second minute, after correcting the former for $Li^8 + He^6$ and the latter for C^{11} decay in 1 minute. Subtraction yielded the apparent C^{10} activity which was used to compute the C^{10} production cross section.

The Be^7 activity was measured in a separate experiment. A small piece of polyethylene was placed against the cyclotron tank window for about ten hours of neutron bombardment. This piece of polyethylene was counted for C^{11} beta activity at a known time after end of bombardment, and was then aged until the C^{11} rate was negligible. Daily and then weekly counts were made on this piece, with and without lead converters. The sample was placed in direct contact with the counter tube window for all counts. The gamma counting efficiency of the counter tube was determined by a side experiment for use in computing the cross section for Be^7 production.

The separation of Li^8 and He^6 activities required absorption technique. The two activities have practically identical half-lives, but do differ in their beta-spectra. It was calculated that 262 mils of aluminum should just stop all the He^6 betas (3.7 Mev maximum), while leaving a fraction of the Li^8 betas (12.8-Mev maximum).
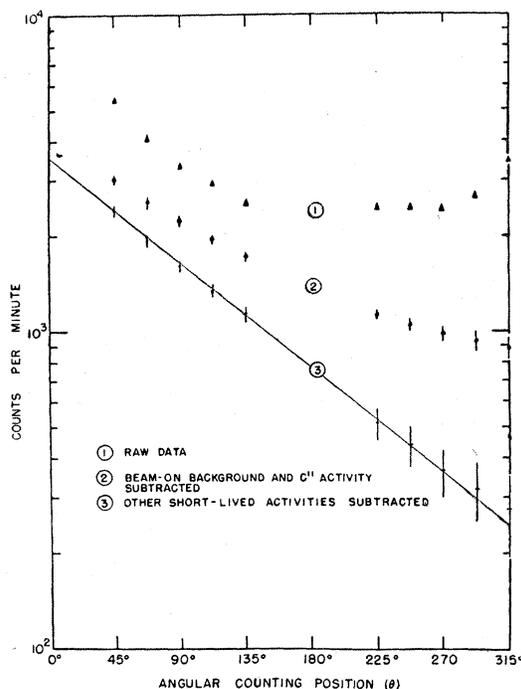
FIG. 4. Typical beta-activity measurements at 600 rpm as a function of counter angular position.

A series of absorbers was used to attenuate the count rate at the 135-degree position of a 60-rpm run.

This was repeated at the 45 degree position of a 60-rpm run to check the effect of the same absorbers on
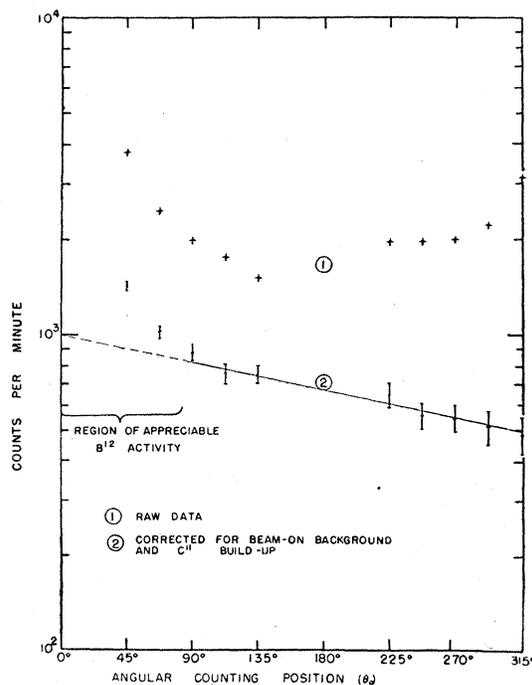
FIG. 5. Typical beta-activity measurements at 60 rpm as a function of counter angular position.

TABLE II. Results of cloud-chamber method. Cross sections expressed in millibarns (10^{-27} cm²), normalized to the n-p cross section.

Star	Number found	Cross section	No. of protons of energy over 20 Mev	No. of deuterons of energy over 27 Mev	No. of tritons of energy over 33 Mev
Two prong:	557	125±10	278	66	7
p B	422	95±9	278		
d B	104	24±4		66	
t B	16	3.6±1.0			7
α Be	11±2	2.5±1.1			
Li Li	4±2	0.9±0.6			
(Unidentified two prong 4)					
Three prong:	318	71±9	68	25	3
α α α	43	9.8±2.0			
He³ α α	5	1.1±0.4			
p α Li	78	17.7±2.5	30		
p He³ Li	7	1.6±0.6	1		
d α Li	46	10.5±2.0		10	
d He³ Li	2	0.4±0.2			
t α Li	6	1.4±0.5			
t He³ Li	4	0.9±0.4			
p p Be	28	6.3±1.5	19		
p d Be	43	9.8±2.0	12	11	
p t Be	13	2.9±0.9	6		1
d d Be	25	5.7±1.3		3	
d t Be	18	4.1±1.0		1	2
Four prong:	151	34±7	32	17	3
p p α α	29	6.6±1.5	11		
p p He³ α	2	0.4±0.02			
p d α α	41	9.3±2.0	10		
p d He³ α	1	0.2±0.2	1		
d d α α	25	5.7±1.3		11	
d t α α	8	1.8±0.6		2	1
d t He³ α	5	1.1±0.4		1	
p t α α	15	3.4±1.0	4		1
p t He³ α	2	0.4±0.2	1		
p p p Li	1	0.2±0.2	2		
p p d Li	7	1.6±0.6	2		
p d d Li	5	1.1±0.4		2	
d d d Li	1	0.2±0.2			
p d t Li	7	1.6±0.6	1	1	1
d d t Li	2	0.4±0.2			
Five prong:	7	1.6±0.6			
p p p d α	2	0.4±0.2			
p p d d α	1	0.2±0.2			
p d d d α	1	0.2±0.2			
p d d t α	3	0.7±0.3			
Total stars 1033		232±17	378	115	13
Heavy fragments:					
B	542	120±12			
Be	304±4	79±9	(This includes presumed Be⁸→2α)		
Li	170±4	44±7			
Singly charged particles:					
p	769	173±15	378		
d	400	90±10		115	
t	96	22±6			13

B^{12} (13.43 Mev maximum) betas. This involved some computation, since the 45 degree position counter saw all three activities—He^6, Li^8, and B^{12}.

The remaining possible products are B^8, Li^9, and Be^{10}. The B^8 and Li^9 cross sections could not have exceeded one millibarn each, judging from the manner in which the 60-rpm activity mixture curves agreed with the theoretical mixture curve of Fig. 3. There was no evidence of any shorter half-life present than that of B^{12}. B^{10} has too long a half-life (2.5×10^6 years) to be detected by this method without unduly long bombardment.

Typical data obtained during runs of the rotating disk are shown in Table IV.

IV. CLOUD-CHAMBER METHOD

The cloud chamber used was of the rubber diaphragm type, with a diameter of 22 inches, and a depth of four inches. The chamber was placed horizontally in a vertical magnetic field of 21 700 gauss produced by a peak current of 4000 amperes pulsed through a pair of Helmholz coils. The composition of the cloud-chamber gas mixture in terms of the expanded partial pressures at 19.5°C was as follows:

methane (99 percent CH_4, 1 percent C_2H_6):	47.45 cm Hg.
hydrogen:	34.85 cm Hg.
water vapor:	1.75 cm Hg.

The stopping power of this mixture was calculated to be 0.645 relative to standard air. Comparisons of $H\rho$ and range for tracks of several particles identified by other means verified this figure to within about ±5 percent. The actual measurements of direction, radius of curvature, range and density of the star tracks were made with the aid of a special stereoscopic double projector.[7] The systematic identification of fragments was greatly facilitated by the use of tables, which constitute UCRL-1445, "Energy and Ionization of Light Particles as a Function of $H\rho$" (by Donald Johnson, August, 1951). An additional variable, range, is readily supplied from range-energies curves.[9]

Normalization of the cross sections determined for various events, products, and reactions was made by use of the neutron-proton scattering cross section. The value 77±1.5 millibarns was adopted for this cross section after careful comparison of the results obtained by Hadley et al.,[3] Brueckner et al.,[7] and others.

The ideal normalization scheme would have been one of counting all proton recoils produced by the beam in a given volume in the cloud chamber, counting all other events produced on the same region, and forming a parallel ratio of cross sections. Since short proton recoils are difficult to identify, an arbitrary cutoff was made at three centimeters, which is the range of a one-Mev proton elastically scattered at 84 degrees (laboratory system) by a 90-Mev incident neutron. This method[7] requires the determination of the fraction of proton recoils lost thereby. This determination, made both analytically and graphically, yielded 1.5±0.5 percent, so the n-p cross section value of 77±1.5 millibarns was replaced by (0.95±0.005) times (77±1.5) or 76±2 millibarns.

[9] Aron, Hoffman, and Williams, U. S. Atomic Energy Commission Report AECU-663, May 28, 1951; University of California Radiation Laboratory UCRL-121 (unpublished).

A final step needed for normalization was the determination of the relative numbers of nuclei of carbon and hydrogen present in the cloud-chamber gas. This was done as follows: Taking the partial gas pressures, one computed the relative numbers of carbon, hydrogen and oxygen nuclei present: carbon 47.925, hydrogen 263.95 oxygen 1.75.

The oxygen necessarily present was a source of error. This error was decreased somewhat by discarding 14 stars identified as oxygen stars. On the basis of the above relative numbers of nuclei, and approximating the oxygen star formation cross section as equal to that of carbon, there should have been about 36 oxygen stars among 1000 stars. Therefore, the relative number for oxygen (1.75) was reduced to $(36-14)/36 \times 1.75$, or 1.07 and then lumped with the carbon number to yield carbon 48.995 and hydrogen 263.95 or a target hydrogen-to-carbon ratio of 5.387. It was now possible to say, for a given reaction X in carbon,

$$\frac{\sigma_X \text{(millibarns)}}{76 \text{ millibarns}} = \frac{\text{number of proton recoils counted}}{\text{(number of events } x \text{ counted)}(5.387)}. \tag{2}$$

The cloud-chamber method yielded a number of cross sections which are shown in the summary of Table II. In presenting the cloud chamber data, the following conventional symbols have been used: p=proton; d=deuteron; t=triton; α, Li, Be, B=helium, lithium, beryllium and boron, respectively, with undetermined mass numbers.

Neutrons leaving the target nucleus are not indicated in this system, since their number is usually undetermined. For example, the notation (p, d, Be) indicates a cloud-chamber star consisting of three prongs—one proton, one deuteron, one beryllium residual nucleus of undetermined mass number, and an undetermined number of neutrons.

V. DISCUSSION OF RESULTS

The cross section for star formation was calculated to be 232 ± 17 millibarns. Adding on the 22 ± 4 millibarns of C^{11} production (not detected in star analysis), one obtained 254 ± 21 millibarns. De Juren and Knable[4] obtained a value of 224 ± 40 millibarns at 95 Mev, which would presumably have become about 237 ± 40 millibarns at 90 Mev. These two results agree within their errors.

A second comparison was made with the data of Hadley and York,[2] as follows.

Product	Protons over 20 Mev	Deuterons over 27 Mev	Tritons over 33 Mev
Cross section (millibarns) (author)	85.3 ± 9.2	26.1 ± 3.4	3.9 ± 0.93
Cross section (millibarns) (Hadley-York)	90 ± 20	26 ± 6	3 ± 0.8

A third comparison made was of the yield of protons over 35 Mev, estimated by Hadley and York to be
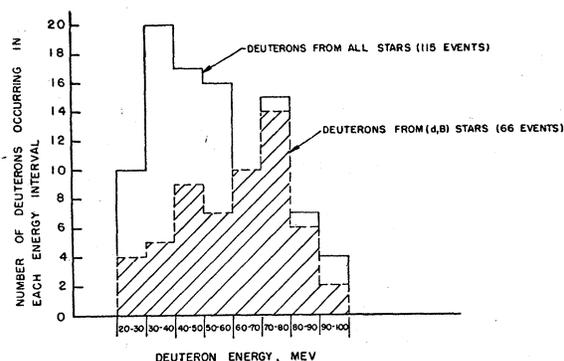
FIG. 6. Energy distribution of high energy deuterons. The total height of each column indicates the number of deuterons occurring in each energy range, while the shaded portion of each column shows how many of these deuterons originated in (d, B) stars.

about 52 millibarns. The value obtained in the present work was 57.5 ± 5 millibarns. This agreement seems to indicate that no appreciable number of protons was lost through mistaking two-prong stars for proton recoils.

An attempt was made to determine the elastic cross section by counting all the short single-prong tracks, and then subtracting the 22 millibarns of C^{11} reaction and the 1 millibarn of "lost" proton recoils. This was not too satisfactory a process, since extremely short tracks were hard to differentiate from the film background. The elastic cross section thus determined was 250 ± 60 millibarns, which is in fair agreement with the value computed from the work of De Juren and Knable,[4] namely 285 ± 25 millibarns, but agrees only because of the rather large error that must be assigned to the measured value. Adding the elastic and inelastic cross sections thus determined yields a value for the total cross section as follows:

star formation:	232 ± 17 millibarns
$C^{12}(n,2n)C^{11}$:	22 ± 4
elastic collision:	250 ± 60
	504 ± 80

which agrees with the value of 520 ± 15 millibarns extrapolated to 90 Mev from the work of De Juren and Knable.[4]

Some deductions can be made to remedy the lack of experimental determinations of the isotopic (mass) numbers of heavy fragments in the cloud-chamber method. This involves mass balancing and a number of assumptions, as follows:

1. Only the following isotopes were assumed possible: $H^{1,2,3}$, $He^{3,4,6}$, $Li^{6,7,8,9}$, $Be^{7,8,9,10}$, $B^{8,10,11,12}$, $C^{10,11,12,13}$.

2. The 1.1 percent of C^{13} present in the target is assumed to undergo reactions in the same manner as C^{12}, and hence not to favor any particular type of reaction. For 90-Mev incident neutrons, this does not seem an unreasonable assumption.

TABLE III. Summary of reactions.

1. Production of carbon isotopes

Reaction	Cross section	Method
$C^{12}(n;n)C^{12}$ (elastic scatt)	275 ± 50 mb	Ref. 4
$C^{12}(n;2n)C^{11}$	22 ± 4 mb	Ref. 1
$C^{12}(n;3n)C^{10}$	0.67 ± 0.50 mb	Rot. disk

2. Production of boron isotopes (two-prong stars)

	Cloud chamber method	Rotating disk method
$C^{12}(n;p)B^{12}$ $(n;p,n)B^{11}$ $(n;p,2n)B^{10}$ $(n;p,4n)B^8$	95 ± 9 mb	4.93 ± 1.0 mb
$C^{12}(n;d)B^{11}$ $(n;d,n)B^{10}$ $(n;d,3n)B^8$	24 ± 4 mb	<1.0 mb
$C^{12}(n;t)B^{10}$ $(n;t,2n)B^8$	3.6 ± 1 mb	

3. Production of Be isotopes (2 and 3-prong stars)

$C^{12}(n;2p,n)Be^{10}$ $(n;2p,2n)Be^9$ $(n;2p,4n)Be^7$	6.3 ± 1.5 mb	
$C^{12}(n;d,p)Be^{10}$ $(n;d,p,n)Be^9$ $(n;d,p,3n)Be^7$	9.8 ± 2 mb	8.8 ± 4.6 mb
$(n;2d)Be^9$ $(n;2d,2n)Be^7$	5.7 ± 1.3 mb	
$C^{12}(n;t,p)Be^9$ $(n;t,p,2n)Be^7$	2.9 ± 0.9 mb	
a$C^{12}(n;t,d,n)Be^7$	4.1 ± 1.0 mb	
$C^{12}(n;\alpha)Be^9$ $(n;\alpha,2n)Be^7$	2.5 ± 1.1 mb	

4. Production of Be⁸*→2α

a$C^{12}(n;\alpha,n)2\alpha$	9.8 ± 2.0 mb
a$C^{12}(n;He^3,2n)2\alpha$	1.1 ± 0.4 mb
a$C^{12}(n;2p,3n)2\alpha$	6.6 ± 1.5 mb
a$C^{12}(n;p,d,2n)2\alpha$	9.3 ± 2.0 mb
a$C^{12}(np2d,n)2\alpha$	5.7 ± 1.3 mb
a$C^{12}(n;p,t,n)2\alpha$	3.4 ± 1.5 mb
a$C^{12}(n;d,t)2\alpha$	1.8 ± 0.6 mb

5. Production of lithium isotopes

$C^{12}(n;3p,n)Li^9$ $C^{12}(n;3p,2n)Li^8$ $C^{12}(n;3p,3n)Li^7$ $C^{12}(n;3p,4n)Li^6$	0.2 ± 0.2 mb
$C^{12}(n;p,He^3)Li^9$ $C^{12}(n;p,He^3,n)Li^8$ $C^{12}(n;p,He^3,2n)Li^7$ $C^{12}(n;p,He^3,3n)Li^6$	1.6 ± 0.6 mb
$C^{12}(n;p,\alpha)Li^8$ $C^{12}(n;p,\alpha,n)Li^7$ $C^{12}(n;p,\alpha,2n)Li^6$	17.7 ± 2.5 mb
$C^{12}(n;d,He^3)Li^8$ $C^{12}(n;d,He^3,n)Li^7$ $C^{12}(n;d,He^3,2n)Li^6$	0.4 ± 0.2 mb
$C^{12}(n;2p,d)Li^9$ $C^{12}(n;2p,d,n)Li^8$ $C^{12}(n;2p,d,2n)Li^7$ $C^{12}(n;2p,d,3n)Li^6$	1.6 ± 0.6 mb
$C^{12}(n;p,2d)Li^8$ $C^{12}(n;p,2d,n)Li^7$ $C^{12}(n;p,2d,2n)Li^6$	1.1 ± 0.4 mb
$C^{12}(n;d,\alpha)Li^7$ $C^{12}(n;d,\alpha n)Li^6$	10.5 ± 2.0 mb
$C^{12}(n;t,He^3)Li^7$ $C^{12}(n;t,He^3,n)Li^6$	0.9 ± 0.4 mb
$C^{12}(n;3d)Li^7$ $C^{12}(n;3d,n)Li^6$	0.2 ± 0.2 mb
$C^{12}(n;p,d,t)Li^7$ $C^{12}(n;p,d,t,n)Li^6$	1.6 ± 0.6 mb
$C^{12}(n;Li^6)Li^7$ $C^{12}(n;Li^6,n)Li^6$	0.9 ± 0.6 mb
a$C^{12}(n;t\alpha)Li^6$	1.4 ± 0.5 mb
a$C^{12}(n;2d,t)Li^6$	0.4 ± 0.2 mb

(Right-side brace annotations: <1.0 mb; 0.82 ± 0.42 mb)

a Denotes unambiguous reactions.

3. The 2.2 percent of O^{16} lumped with C^{12} is also assumed to favor no particular reaction.

4. It is estimated that no free neutron (including the incident neutron) leaves the target nucleus in about ten percent of all reactions in which at least one charged particle is knocked out.

This estimate is arrived at as follows:

a. The 5 millibarn yield for $C^{12}(n;p)B^{12}$ found by the rotating disk method, compared to the 95 millibarn yield for (p, B) stars found by the cloud-chamber method indicates that about five percent of the incident neutrons which knock out single protons remain trapped in the residual boron nucleus.

b. In the case of (d, B) stars, a plot of the energy distribution of the high energy deuterons (over 27 Mev) shows a distinct peak at about 70 Mev, and a lower broad maximum at about 30 to 40 Mev. The higher peak is assumed to be due to deuteron pick-up with no free neutron leaving the nucleus, while the lower maximum is assumed to be due to a spallation with neutron emission. A rough resolution into these two classes (limited by the presence of only sixty-six pertinent events in over a thousand stars) would seem to indicate that about one-third of the high energy (over 27 Mev) deuterons are emitted by pick-up, and therefore about 20 percent (about 5 millibarns) of all (d, B) stars were accompanied by no emitted neutrons. See Fig. 6.

c. In the case of deuterons emitted in stars of type other than (d, B), the low deuteron energies found as a rule seem to indicate very few pick-up processes (presumably followed by spallation) if any; it is doubtful

that the subsequent spallations required in such cases (to produce the fragments seen) would not result in neutron emission.

d. In the case of (t, B) stars, the triton energy distribution seems to indicate that about half (1.8 millibarns) of these occurred by pick-up with no neutron emission.

e. If Be^8 is assumed to be the intermediate step for production of alpha-pairs, then the 1.8±0.6 millibarns of $(d, t, 2\alpha)$ stars occur with no neutron emission.

f. The two unambiguous reactions $C^{12}(n;t,\alpha)Li^6$ and $C^{12}(n;2d,t)Li^6$ give 1.8±0.7 millibarns of no neutron emission.

The above reactions, especially the pick-up and n–p processes, are the more likely ones to give no neutron emission, and yield about 15 millibarns of no neutron emission out of 250 millibarns worth of inelastic events, i.e., about six percent. Allowing an increment for undetected no-neutron emissions among the other reactions in accordance with (b) and (c) raises the estimate to about ten percent.

It is now possible to make some deductions regarding yields of specific heavy isotopes:

1. The 4.1±1.0 millibarn cross section for (d, t, Be) stars is the minimum possible cross section for Be^7 production. (Assumptions 1, 2, and 3 or 4 alone.)

2. If all four assumptions are used, the greatest part of the following cross sections may be added to give a new and higher estimate of Be^7 cross section:

$$(d, d, Be) \text{ stars} - 5.7\pm1.3 \text{ mb},$$
$$(p, t, Be) \text{ stars} - 2.9\pm0.9 \text{ mb},$$
$$(\alpha, Be) \text{ stars} - 2.5\pm1.1 \text{ mb}.$$

The final result is 14.5±4.3 millibarns for the Be^7 production cross section which is to be compared with the rotating disk method value of 8.8±4.6 millibarns.

3. The maximum Be^{10} cross section is 16.1±3.5 millibarns if assumption 4 is not used, but drops to 6.8±1.6 millibarns if assumption 4 is used; this latter value is the most probable cross section.

4. Using all four assumptions, Be^9 is assigned a maximum yield of 15±3.5 millibarns.

5. The yield of Be^8 (as an intermediate nucleus in the process of making two alphas) is assigned a maximum value of 26±4 millibarns.

6. Using all four assumptions, Li^8 is assigned a maximum yield of 3.4±1.4 millibarns. This includes a maximum possible yield of 0.2±0.2 millibarn of Li^9. The value for Li^8 is higher than the experimental result of 0.8±0.4 millibarn found by the rotating disk method, but does not necessarily contradict it, since the deduced result is a maximum. The deduced Li^9 yield agrees with that from the rotating disk method (<1 millibarn).

7. The representative yields of Li^7 and Li^6 cannot be deduced from the evidence at hand. The sum of Li^7 and Li^6 yields is about 40 millibarns.

TABLE IV. Yield of heavy fragments.

Fragment	Cross section, rotating disk method	Cross section, cloud-chamber method
C^{10}	0.67±0.50 mb	...
B^{12}	4.93±1.0 mb	...
B^{11}	...	}118±13 mb
B^{10}	...	
B^8	<1.0 mb	...
Be^{10}	...	6.8±1.6 mb
Be^9	...	15±3.5 mb
$Be^8*(\rightarrow2\alpha)$	...	26±4 mb
Be^7	8.8±4.6 mb	14.5±4.3 mb
Li^9	<1.0 mb	0.2±0.2 mb
Li^8	0.82±0.42 mb	3.4±1.4 mb
Li^7	...	}40±7 mb
Li^6	...	
He^6	2.54±0.96 mb	...

8. In the case of boron isotopes, the rotating disk method furnished 4.93±1.0 millibarns for B^{12} and <1 millibarn for B^8 yield, but the present analysis discloses no breakdown of the 115 millibarns of B^{11} plus B^{10} yield.

9. No deductions can be made from the cloud chamber results concerning He^6 yield; the rotating disk method result was 2.54±0.96 millibarns.

See Tables III and IV for a summary of the deductions made in this section.

VI. CONCLUSIONS

The cross sections determined by the two methods cover the possible reactions induced in carbon by 90-Mev neutrons. In the case of the cloud-chamber method, only limited and approximate identifications of heavy fragments could be made as regards their mass numbers. The rotating disk method, however, filled in this data in the case of several radioactive products, with the notable exception of Be^{10}.

The mechanisms by which high and low energy singly charged particles (protons, deuterons, and tritons) are produced were compared. Of the high energy singly charged particles (protons over 20 Mev, deuterons over 27 Mev, tritons over 33 Mev), 74 percent of the protons, 57 percent of the deuterons and 50 percent of the tritons were produced from two-prong stars (by knock-on or pick-up); the remainder came from multifragment stars or spallations.

It is, therefore, noteworthy how well the yields for p, B stars (95±9 millibarns), d, B stars (24±4), and t, B stars (3.6±1) agree numerically with the yields for high energy protons (95±9), deuterons (26±3) and tritons (3±1) from all reactions.

The total proton, deuteron and triton yields, of all energies and from all reactions, were 172.5±15, 89.5 ±10, and 21.5±6 millibarns respectively, showing a greater preponderance of deuterons and tritons relative to protons than was the case in the yields of high energy singly charged particles.

It can be stated with some assurance that Li⁸ is present as a residual nucleus, that the splitting of carbon into three alpha-particles does occur with 90-Mev neutrons, and that carbon does split into two heavy fragments (Li, Li or α, Be).

The cross sections measured by Hadley and York have been verified and extended to encompass lower energy singly charged particles.

Spin Interactions of Accelerated Nuclei in Molecules

NORMAN F. RAMSEY
Harvard University, Cambridge, Massachusetts
(Received December 31, 1952)

The contributions to the spin-rotational magnetic interaction of a nucleus in a molecule of terms dependent on the acceleration of the nucleus are calculated. One of these arises from the fact that the acceleration in molecules is electrical and the moving nuclear magnetic moment interacts with the electric field. The other is the Thomas precession similar to that which occurs for electrons in atoms. The effects of both centripetal acceleration and zero-point vibration acceleration are considered; the latter produces the largest effect. A general expression for the combined effect of these terms is given. When it is averaged over the zero point vibration of the H_2 and D_2 molecules, the contribution to the spin-rotational interaction constant c is 1059 cps for H_2 and 30.6 cps for D_2.

I. INTRODUCTION

IN his theory of the spin-rotational magnetic interaction of a nucleus in a molecule, Wick[1] assumes that the interaction arises exclusively from the magnetic field which results from the circulation of the other charges in the rotating molecule. Although this assumption is approximately valid, an appreciable correction is required when the effects of the acceleration of the nucleus are considered. One of these effects is that the acceleration of the nucleus in the molecule is caused by an electric field and the moving nuclear magnetic moment interacts with this field. The other is the Thomas precession. The accelerations producing these effects arise from two sources: the rotation of the molecule and the zero-point vibration in the molecule. Although for each of these the average acceleration is zero, they nevertheless contribute to the spin-rotational magnetic interaction as is discussed in the following paragraphs.

II. INTERACTIONS

Since the acceleration of a nucleus in the molecule is caused by an electric field, a nucleus of mass M whose acceleration is $d\mathbf{v}/dt$ must be acted on by an electric field, $\mathbf{E}$, which is given by

$$M d\mathbf{v}/dt = Ze\mathbf{E}. \qquad (1)$$

However, to the nucleus moving with velocity $\mathbf{v}$ through this electric field, there will appear to be a magnetic field

$$\mathbf{H}_E = \mathbf{E} \times \mathbf{v}/c. \qquad (2)$$

If the nucleus has a gyromagnetic ratio γ, it will precess in this magnetic field with the angular frequency

$$\omega_E = -\gamma \mathbf{H}_E = -\gamma \mathbf{E} \times \mathbf{v}/c. \qquad (3)$$

In addition, there will be the purely kinematical Thomas precession[2,3]

$$\omega_T = (d\mathbf{v}/dt) \times \mathbf{v}/2c^2 = (Ze/2Mc)\mathbf{E} \times \mathbf{v}/c, \qquad (4)$$

where the last step comes from Eq. (1). The total precessional frequency, ω_A, due to the nuclear acceleration is therefore

$$\omega_A = -\gamma[1 - (Ze/2Mc\gamma)]\mathbf{E} \times \mathbf{v}/c. \qquad (5)$$

Since the discussion of nuclear precession frequencies is usually given in terms of the Hamiltonian of the system which gives rise to these precession frequencies, it is convenient to express the result in the form of a term $\mathfrak{IC}_A$ of the nuclear Hamiltonian which will give rise to the precession frequency of Eq. (5). If the nucleus has the spin angular momentum $\mathbf{I}$, in units of $\hbar$, this precessional frequency will result if

$$\mathfrak{IC}_A = \hbar \mathbf{I} \cdot \omega_A = -\hbar\gamma[1 - (Ze/2Mc\gamma)]\mathbf{I} \cdot (\mathbf{E} \times \mathbf{v}/c). \qquad (6)$$

From this it is apparent that even though $\mathbf{E}$ is zero on the average, it makes a resultant contribution since it is the average value of $\mathbf{E} \times \mathbf{v}/c$ and not of $\mathbf{E}$ that is important. When $\mathbf{E}$ results from centripetal stretching it is clear that $\mathbf{E} \times \mathbf{v}/c$ has a net average value since it

¹ G. C. Wick, Phys. Rev. **73**, 51 (1948).

² L. H. Thomas, Phil. Mag. **3**, 1 (1926).
³ H. C. Corben and P. Stehle, *Classical Mechanics* (John Wiley and Sons, Inc., New York, 1950).